Evaluation of the bioactive properties of avenanthramide analogs produced in recombinant yeast

UNIVERSITÀ DEGLI STUDI DI TORINO

Evaluation of the bioactive properties of avenanthramide analogues produced in recombinant yeast

Moglia Andrea[a,g], Goitre Luca[b,g], Gianoglio Silvia[a,g], Baldini Eva[c,g], Trapani Eliana[b,g], Genre Andrea[d], Scattina Antonella[e], Dondo Giancarlo[e], Trabalzini Lorenza[c,g], Beekwilder Jules[f], Retta Saverio Francesco[b,g*]

[a] Department of Agricultural, Forest and Food Sciences, Università degli Studi di Torino, Largo Paolo Braccini 2, 10095 Grugliasco (Italy).

[b] Department of Clinical and Biological Sciences, Università degli Studi di Torino, Regione Gonzole 10, 10043 Orbassano (TO).

[c] Department of Biotechnology, Chemistry and Pharmacy, Università degli Studi di Siena, Via Aldo Moro 2, 53100 Siena.

[d] Department of Life Sciences and Systems Biology, Università degli Studi di Torino, Viale Mattioli 25, 10125 Torino.

[e] Active Cells Srl, c/o CBA Largo R. Benzi, 10, 16136 Genova.

[f] Plant Research International, P.O. Box 16, 6700 AA Wageningen (The Netherlands).

[g] CCM Italia research network (www.ccmitalia.unito.it).

[*]Corresponding author:

Retta Saverio Francesco

Tel: +39 011.6706426; Fax: +39 011.9038639

E.mail address: francesco.retta@unito.it

Running title: Bioactive effects of yeast avenanthramides

Abstract

Saccharomyces cerevisiae has been proven to be a valuable tool for the expression of plant metabolic pathways. By engineering a *S. cerevisiae* strain with two plant genes (*4cl-2* from tobacco and *hct* from globe artichoke) we previously set up a system for the production of two novel phenolic compounds, N-(E)-*p*-coumaroyl-3-hydroxyanthranilic acid (Yeast avenanthramide I, Yav I) and N-(E)-caffeoyl-3-hydroxyanthranilic acid (Yeast avenanthramide II, Yav II). These compounds have a structural similarity with a class of bioactive oat compounds called avenanthramides.

By developing a fermentation process for the engineered *S. cerevisiae* strain, we obtained a high-yield production of Yav I and Yav II. To examine the biological relevance of these compounds, we tested their potential antioxidant and antiproliferative properties upon treatment of widely used cell models, including immortalised mouse embryonic fibroblast (MEF) cell lines and the HeLa cancer cells. The outcomes of our experiments showed that both Yav I and Yav II enter the cell and trigger a significant up-regulation of master regulators of cell antioxidant responses, including the major antioxidant protein SOD2 and its transcriptional regulator FoxO1, as well as the down-regulation of Cyclin D1. Intriguingly, these effects were also demonstrated in cellular models of the human genetic disease Cerebral Cavernous Malformation (CCM), suggesting that the novel phenolic compounds Yav I and Yav II are endowed with bioactive properties relevant to biomedical applications.

Taken together, our data demonstrate the feasibility of biotechnological production system of yeast avenanthramides and underline a biologically relevant antioxidant activity of these molecules.

Keywords: *Saccharomyces cerevisiae*, metabolic engineering, avenanthramides, plant secondary metabolites, phenolic compounds, biofactors, antioxidants, Cerebral Cavernous Malformation (CCM)

1 Introduction

The notion that plant secondary metabolites provide greater opportunity for drug discovery and development than purely synthetic approaches has been well established. These molecules have an important function for human health, because they can act as strong antioxidant and anti-inflammatory agents, and can exert anti-cancer chemoprotective activities.

Plant secondary metabolites can be produced mainly by chemical synthesis or by extracting them directly from cultivated or wild plants. Chemical synthesis of secondary metabolites presents many advantages, such as high yield rates; however, it is strongly hindered by the complexity of the molecules and the large quantities of expensive and non-ecofriendly chemicals required. Extraction of secondary metabolites from plant sources is often limited by low abundance and environmental, seasonal as well regional variations [1].

Heterologous production of secondary metabolites in recombinant microorganisms represents an attractive strategy to increase and optimize both the production of natural occurring compounds of therapeutic interest and new emergent compounds [2-6]. In particular, the *S. cerevisiae* yeast-based expression system offers several advantages over chemical synthesis or direct extraction from plant tissue, because of its ease of manipulation and cultivation as well as its safety and abundant knowledge about genetics, physiology and fermentation techniques. Additional advantages of *S. cerevisiae* consist in its capability for protein processing typical of eukaryotic organisms, such as protein folding and post-translation modifications, thus being a useful system for heterologous expression of plant secondary metabolites endowed with biological properties relevant to biomedical applications.

Remarkable examples of pharmaceutical metabolites produced in recombinant yeast strains expressing plant genes include the precursor of the antimalarial drugs artemisinic acid and taxadiene [7-10], flavonoids [11-13], vitamin C [14], hydrocortisone [15], serotonin derivates [16], resveratrol [17-20], valencene [21], ginsenoids [22].

A novel system for the heterologous production of two antioxidative phenolic amides, N-(E)-*p*-coumaroyl-3-hydroxyanthranilic acid (Yeast avenanthramide I, Yav I) and caffeoyl-3-hydroxyanthranilic acid (Yeast avenanthramide II, Yav II), was set up by engineering a *S. cerevisiae* strain with two genes (*4cl-2* from tobacco and *hct* from globe artichoke) encoding key proteins involved in the biosynthesis of phenolic esters [23] (Figure 1). These novel compounds showed a strong structural similarity with avenanthramides, a group of hydroxycinnamoylanthranilates that constitute the main soluble phenolic compounds in oat kernels. Radical-scavenging activity has been shown for a wide range of avenanthramides *in vitro*, as well as antioxidant and anti-inflammatory activities [24-26]. Consistently, previously we showed that yeast avenanthramides possess strong antioxidant activity when tested in $ABTS^{\bullet+}$ radical quenching assay, as well as the capacity to reduce the intracellular levels of reactive oxygen species (ROS) in a cellular antioxidant assay (CAA) based on mouse embryonic fibroblast (MEF) cell models [23].

Here we report the characterization of bioactive properties of yeast avenanthramides produced in *S. cerevisiae* through fermentation approach. We show that these novel phenolic compounds can modulate the expression levels of master regulators of cell antioxidant and proliferative responses, including the up-regulation of the FoxO1-SOD2 antioxidant pathway and the down-regulation of Cyclin D1. In addition, these effects were also demonstrated in cellular models of the human genetic disease Cerebral Cavernous Malformation (CCM), suggesting that these compounds are endowed with biological properties relevant to biomedical applications.

2 Materials and Methods

2.1 The pESC-URA-4CL-HCT plasmid

The globe artichoke *hct* gene (accession DQ104740) was PCR amplified from the plasmid pGEM-HCT using primers 5'-TCTGGATCCATGAAGATCGAGGTGAGAGAA and 5'-TCTGGTACC TTAGATATCATATAGGAACTTGC and the resulting amplicon was digested with *BamHI* and *KpnI* and ligated into linearized pESC-URA vector (Agilent). The tobacco *4cl-2* gene [27] was PCR amplified using primers 5'-TCTGAATTCATGGAGAAAGATACAAAACAGG and 5'-TCTGCGGCCGCTTAATTTGGAAGCCCAGCAG and the resulting amplicon was digested with *EcoRI* and *NotI* and ligated into linearized pESC-URA-HCT vector.

The resulting pESC-URA-4CL-HCT plasmid was introduced into *S. cerevisiae* CEN.PK113-5d (*ura*3), so that 4CL and HCT were under the control, respectively, of the galactose GAL 10 and GAL 1 promoters. The transformation of *S. cerevisiae* strain was achieved using the lithium acetate / single strand carrier DNA / polyethylene glycol method [28]. Transformants were selected on Synthetic Dextrose (SD) minimal medium (0.67% yeast nitrogen base medium without amino acids, 2% D-glucose, 2% agar from SIGMA) supplemented with amino acids, but omitting Uracil for auxotrophic selection of transformants. The success of the transformation was confirmed by PCR analysis.

Single colonies of transformed yeast strain were transferred to 5 mL YPD medium at 30°C for 20 h with shaking (250 rpm). Overnight culture was diluted 1:25 in 50 mL of fresh YPD medium and cultured at 28°C in the presence of 2% galactose to induce transgene expression. When the OD_{600} reached 0.4, *p*-coumaric acid (3 mM) or caffeic acid (3 mM) and 3-hydroxyanthramilic acid (500 µM) (SIGMA) were added.

2.2 Fermentation process

Seed cultures for bioreactors were prepared by inoculating frozen cells in 25% (v/v) glycerol into SD agar plates for 3 days at 30°C. 10 mL of the resuspended yeast cells (Wickerman scale value=3) were used to inoculate two 2 L flasks containing 600 mL of YPD pre-fermentation medium formulated as

follows: 6 g/L bactopeptone (BD), 14 g/L peptone (Costantino), 10 g/L yeast extract (Costantino), 2% D-glucose (SIGMA), antifoaming (SIGMA); final pH 6.6±0.1. These flasks were grown for 20 h at 30°C (160 rpm), and then 1.2 L of the yeast culture were used to inoculate 14 L of YPGal fermentation medium formulated as follows: 6 g/L bactopeptone, 14 g/L peptone, 10 g/L yeast extract, 20 g/L galactose (SIGMA), antifoaming. The pH was corrected to a final value of 6.6±0.1.

Fermentation took place in a 15 L fermentor (B. Braun Biostat C): pH was controlled automatically and maintained in the range 4.8-6, temperature was kept in the range 29±1°C, dissolved oxygen was maintained at 60%, rpm value varied from 200 to 350 in relation to dissolved oxygen. After 3 h from the beginning of fermentation process, *p*-coumaric acid or caffeic acid (3 mM) and 3-hydroxyanthranilic acid (500 μM) were added. Fermentation continued for 69 h and was sampled periodically for growth (OD600), viability and production titer.

2.3 Extraction and purification of yeast avenanthramides

The supernatant of 15 L culture was extracted 15 L of ethyl acetate. Ethyl acetate phases were pooled and material was concentrated through the use of Rotavapor. Thin Layer Chromatography was performed on aluminium-backed plates pre-coated with silica (0.2 mm, Merck DC-alufolien Kieselgel 60 F254) in the following solvent: chloroform/methanol/acetic acid/water (80/20/2/0,2, v/v/v/v). Flash chromatography was performed on Merck Kieselgel 60 H silica using chloroform/ methanol/acetic acid/water (80/20/2/0,2, v/v/v/v) as solvents.

The yeast avenanthramide content was quantified by reverse-phase HPLC, using an analytical Luna C18 column (2 mm x 150 mm, particle size 3 μm, 100Å; Phenomenex, Torrance, California, USA), along with a 2 mm x 4 mm pre-column (Phenomenex). The mobile phases consisted of a 1:1000 (v/v) mix of degassed glacial acetic acid: ultrapure water (Eluant A) and a 1:1000 (v/v) mix of glacial acetic acid: acetonitrile (Eluant B). The elution gradient started at 5% B: 95% A, and increased linearly to 35% B: 65% A over 28 min. The column was equilibrated with 100% A between injections. The flow rate was 0.5 mL/min and the output was monitored at 300 nm and 330 nm.

2.4 Chemicals

Stock solutions of purified yeast avenanthramides (Yav I and Yav II) and avenanthramide B (Av B, kindly provided by Dr. Collins, Eastern Cereals and Oilseeds Research Center, Ottawa) were prepared by dissolving compounds in dimethil sulfoxide (DMSO) to a final concentration of 0.1 M. Caffeic acid and *p*-coumaric acid were obtained from SIGMA.

2.5 Cell Culture and MTT cell viability assay

HeLa and MEF (mouse embryonic fibroblast) cells, including either wild-type MEFs, KRIT1$^{-/-}$ MEFs ($K^{-/-}$) and KRIT1$^{-/-}$ MEFs re-expressing KRIT1 (K9/6) [29] cells were cultured in high glucose Dulbecco's Modified Eagle Medium (DMEM) supplemented with 10% FBS, 2 mM glutamine and 100 U/ml penicillin/streptomycin at 37°C, 5% CO_2. To perform the MTT viability assay, HeLa cells were seeded in 96 well plates, with a cell density of 5000 cells/well and let adhere to the wells. Cells were then treated with Yav I, Yav II and Av B at four different concentrations: 25 μM, 50 μM, 100 μM and 150 μM. Cells treated with 0.15% dimethylsulfoxide (DMSO) were used as control. After 24 h of incubation, 5 mg/ml MTT reagent was added to the wells and incubated for 3,5 h at 37°C, 5% CO_2. Following the incubation, MTT solution was removed from each well and replaced with 200 μL of DMSO. Absorbance was measured at 550 nm using the microplate reader Multiskan Ascent (Thermo). Avenanthramide-treated cells were compared to control cells and results of cell viability data were expressed as percentage of control cells. Data were normalized for each experiment and treatment differences were analyzed by Student's *t*-test.

2.6 Confocal imaging

Cells grown in complete culture medium were either mock-treated or treated with yeast avenanthramides, Yav I or Yav II, for 24 h. Cells were then imaged using a Leica TCS-SP2 microscope equipped with a 40X water immersion objective. The 405 nm diode was used for Yav I/Yav II

excitation and images were recorded at 420-500 nm as either single optical sections or stacks encompassing the whole cell thickness. Bright-field images were also acquired and superimposed to fluorescence images. Cells were also treated with equivalent concentrations of *p*-coumaric acid or caffeic acid and imaged following the same experimental conditions.

Instrument parameters for sequential image acquisition, including pinhole diameter, laser intensity, exposure time, PMT gain and offset, were set and held constant to minimize autofluorescence and for proper comparison between samples.

2.7 Real-Time PCR

HeLa and MEF cells were grown in complete DMEM up to about 80% confluence and then either treated for 24 h with different concentrations of Yav I, Yav II and Av B in a 0.15% DMSO solution, or mock-treated with equal volumes of 0.15% DMSO.

DNA-free RNA was obtained by purification from cell monolayers using the Pure Link RNA Mini Kit (Invitrogen) and used for the cDNA synthesis with the MMLV Reverse Transcriptase 1st-Strand cDNA Synthesis Kit (Euroclone). Primers (Table 1) were designed on the basis of CDS sequence using the Primer 3 software (http://bioinfo.ut.ee/primer3-0.4.0/). As a housekeeping gene, GAPDH was chosen for its stability and level of expression, which is comparable to the genes of interest and whose expression remained stable after cell treatment.

The cDNA was diluted to obtain a threshold cycle (CT) value between 25 and 32. The 20 µL RT-qPCRs, performed in three biological replicated, contained GoTaq(R) qPCR Master Mix (Promega), 10 µM primer and 3 µL diluted cDNA. PCR reactions were carried out in 48-well optical plates using the iCycler Real-time PCR Detection System (Bio-Rad Laboratories, USA). PCR conditions comprised an initial incubation of 95°C/5min, followed by 35 cycles of 95°C/15s and 60°C/45s. In all experiments, appropriate negative controls containing no template were subjected to the same procedure to detect or exclude any possible contamination. Melting curve analysis was performed at the end of amplification. Standard curves were analyzed using iCycler iQ software. Amplicons were

analyzed by the comparative threshold cycle method, in which ΔΔCt is calculated as ΔCtI- ΔCtM, where ΔCtI is the Ct value for the any target gene normalized to the endogenous housekeeping gene and ΔCtM is the Ct value for the calibrator, which is also normalized to housekeeping gene. Data were normalized for each experiment and treatment differences were analyzed by Student's *t*-test.

2.8 Western blotting analysis

HeLa and MEF cells were grown in complete DMEM up to about 80% confluence and then either treated for 24 h with different concentrations of Yav I, Yav II and Av B in a 0.15% DMSO solution or mock-treated with 0.15% DMSO. Cells were lysed and total cell lysates were analyzed by Western blotting as previously described [30]. Briefly, cell lysates containing equal amounts of total proteins (~50 μg) were separated by either 10% or 12% SDS-PAGE and electro-blotted onto nitrocellulose transfer membrane (Whatman, GE Healthcare). The blots were blocked with 5% milk in Tris-buffered saline (TBS) for 1 h at 37°C, incubated with appropriate dilutions of primary antibodies overnight at 4°C and subsequently with HRP-conjugated secondary antibodies for 1 h at room temperature. The following antibodies were used: rabbit polyclonal antibodies (pAb) against FoxO1 (C29/H4 2880 Cell Signaling), SOD2 (Abcam), tubulin (T5168 Sigma). Primary antibodies were detected using affinity purified HRP-conjugated secondary antibodies (Abcam). To compare the density of protein bands of interest and test for significant differences between samples in Western blotting experiments, blots were scanned and quantified using ImageJ software (http://rsb.info.nih.gov/ij/index.html). Band optical density values (mean±SD) were expressed as relative protein level units and plotted in representative histograms showed in figures.

3 Results

3.1 Yeast avenanthramide production

In order to enable the production of yeast avenanthramides, the *4cl-2* gene from tobacco and the *hct* gene from globe artichoke were introduced into *S. cerevisiae*. To this end, a DNA episomal plasmid containing the tobacco *4cl-2* gene under control of the GAL10 promoter, the globe artichoke *hct* gene under control of the GAL1 promoter, and the selectable marker URA-3 was constructed. The episomal vector pESC-URA-4CL-HCT was used to transform the *S. cerevisiae* CEN.PK113-5d (*ura*3) strain.

This strain was then compared to untransformed yeast (control) for metabolizing phenolic acids added to the YPGal medium in shake flask culture. Specifically, the yeast strain 4CL-HCT was grown for 72 h in the presence of either *p*-coumaric or caffeic acid (3mM) and 3-hydroxyanthranilic acid (500 μM), and the medium was analysed by reverse HPLC.

Metabolic analyses revealed the formation of a peak in both incubation assays, which was not present in control cultures. Chromatographically separated compounds were preliminary identified on the basis of their absorbance spectrum, retention time (rt) and the exact mass of the pseudomolecular ion. In the incubation of 4CL-HCT yeast with *p*-coumaric acid, the peak eluting at rt ~ 24 was identified as N-(E)-*p*-coumaroyl-3-hydroxyanthranilic acid (Yeast avenanthramide I, Yav I, Figure 1 and Supplementary Figure S1).

Likewise, incubation of the 4CL-HCT yeast with caffeic acid resulted in the accumulation of a compound (rt ~21) which was identified as caffeoyl-3-hydroxyanthranilic acid (Yeast avenanthramide II, Yav II, Figure 1 and Supplementary Figure S1) on the basis of rt, absorbance spectrum and molecular mass. Among the different media tested in shake flask cultures, YPGal medium resulted the best in terms of yeast growth and avenanthramide production.

In order to obtain higher yield of yeast avenanthramide production, fermentation of strain 4CL-HCT was performed in a 15L fermentor, with pH controlled in a range from 4.8 to 6.2. In the incubation with both substrates (*p*-coumaric acid and caffeic acid), cell growth reached stationary phase after 24

h reaching a maximum OD_{600} value of 65.7 (Table 2). Yeast avenanthramide production continued to increase until 69 h in both incubation assays, when the highest substrate consumption and Yav I and Yav II production were observed (Figure 2). The production of yeast avenanthramides reached a final yield of 120 mg/L Yav I and 22 mg/L Yav II after 69 h.

3.2 Yav I and Yav II do not affect cell viability

Using a MTT cell viability assay, we found that Yav I and Yav II didn't significantly inhibit the viability of HeLa cells at concentrations up to 150 μM (p>0.05, Figure 3). Notably, the same result was obtained with Av B, in agreement with previously published data [31]. Furthermore, consistent with a previous report [32], the concentration of DMSO used in our assays didn't affect cell viability. The outcomes of the MTT assays suggested that the concentration range 25-150 μM of both Yav I and Yav II was suitable to be used in experiments aimed at analyzing the antioxidant and antiproliferative effect of these compounds.

3.3 Yavs enter the cells and accumulate into cytosolic regions

Using confocal fluorescence microscopy, we found that incubation of HeLa cells with 150 μM Yav II for 2, 24 and 48 h resulted in accumulation of fluorescence into the cells when observed under 405 nm light (Figure 4), indicating that i) the molecule is rapidly taken up by the cells in a sufficient quantity to grant its visualization and ii) maintains its autofluorescence after uptake. Intracellular Yav autofluorescence localized into cytosolic regions and was totally excluded from the nucleus (Figure 4 A-D). Moreover, it reached a maximum intensity after 2 h of cell treatment (Figure 4A, B), and lasted for more than 24 h (Figure 4C, D), although at gradually reduced intensities suggesting that Yav was efficiently uptaken by the cells within 2 h of incubation and persisted at significant levels for at least 24 h before being progressively metabolized. Furthermore, cell treatments with various concentrations of Yavs resulted in proportional intracellular fluorescence accumulation, suggesting a

good cellular uptake of Yavs and a consequent dose-dependent bioavailability. Fluorescence was also observed upon cell incubation with Yav I, although its intensity was lower than in Yav II treated cells (data not shown), suggesting that either Yav I uptake is less efficient or its autofluorescence is less intense compared to Yav II. In contrast, no significant autofluorescence signals were detected in HeLa cells before treatment with Yav compounds (0 h).

To address whether the fluorescence observed upon cell treatments with Yavs derived from either these compounds or their potential metabolic products, we compared fluorescence images of HeLa cells treated with Yavs or either *p*-coumaric acid or caffeic acid, two major potential metabolic products of Yav I and II, respectively. The outcomes of these experiments showed that cell treatment with *p*-coumaric acid or caffeic acid did not lead to significant accumulation of fluorescence (Supplemental Figure S2), indicating that the long-lasting fluorescence observed upon cell treatment with Yavs cannot be attributed to these metabolic products, and suggesting that it is indeed derived directly from Yavs. Furthermore, although it is not possible to exclude that other metabolic products of Yavs may be generated and play a role in Yav-dependent effects, these results support the possibility that the main active compounds of bioactivities are Yavs. Accordingly, the well-established bioactivities of natural avenanthramides from oats, including their antioxidant, anti-proliferative, and anti-inflammatory activities, have been attributed to the native compounds and not to their metabolic products.

3.4 Yavs trigger the expression of master regulators of cell antioxidant responses

To test the effects of Yavs on the regulation of cellular antioxidant defense systems, we performed real-time PCR analysis of the expression levels of two major antioxidant genes, SOD2 and FoxO1, both in HeLa and MEF cells (Figure 5 and 6). Superoxide dismutase (SOD) enzymes play primary roles in protecting and preserving cells against oxidative stress via the scavenging of the superoxide anion, a precursor of all reactive oxygen species. Preliminary time-course experiments at different

time-points (8, 12, 18, 24 and 48 h) allowed us to choose treating cells for 24 h, as this time-point appeared to display the greatest biological effects without any cytotoxic effect.

The outcomes of our experiments showed that the expression of SOD2 was significantly increased in HeLa cells treated with 100 μM Yav I, Yav II and Av B (Figure 5A). Indeed, compared with the control, treatment with 100 μM Yav I and Yav II increased the SOD2 mRNA levels by 2.32 and 3.18 fold, respectively, whereas treatment with Av B led to a lower increase (1.67 fold). Furthermore, a marked up-regulation of SOD2 expression level was observed in MEF cells (Figure 5B). Specifically, the greatest effects were observed after MEF cell treatment with 150 μM Yav I, which induced a 5.8 fold up-regulation, and 100 μM Yav I (4.21 fold). The treatment with Yav II and Av B induced a 3 fold up-regulation.

Among the regulators of ROS levels, the FoxO family has been demonstrated to play a key role through the control of the expression of antioxidant proteins, including catalase and SOD2 [29].

Using quantitative real-time PCR we found that FoxO1 mRNA levels were up-regulated in HeLa cells treated with 100 and 150 μM Yavs, with 100 μM Yav II being the most effective (2.28 fold FoxO1 mRNA level increase), whereas the same concentration of Yav I and Av B induced a 1.9 fold increase of FoxO1 mRNA levels (Figure 6A). Moreover, the outcomes of experiments with MEF cells showed that the expression of FoxO1 was significantly higher in MEF cells treated with 100 μM of Yav I and Av B (Figure 6B). Indeed, compared with the control the FoxO1 mRNA levels were increased by 4.05 and 2.63 fold, respectively. Significant changes were also detected upon Yav II treatments, although to a lower extent. In contrast, catalase mRNA levels were not significantly affected by Yav treatment (data not shown).

To test whether the Yav-induced up-regulation of FoxO1 and SOD2 occurred also at the protein levels, we performed Western blotting of cell extracts from Yav treated cells using monoclonal antibodies specific for FoxO1 and SOD2 as described previously [29]. The outcomes of these experiments showed that Yav treatment resulted in a significant increase of FoxO1 protein levels in both HeLa (Figure 7A,B) and MEF (Figure 7C,D) cells, which was accompanied by a significant up-

regulation of SOD2 protein levels (Figure 7C,D). However, differences in Yav dose-response effects in HeLa and MEF cells were also observed, suggesting that Yavs may exert dose- and cell context-dependent effects similarly to most exogenous antioxidants [33].

3.5 Yavs promote the down-regulation of Cyclin D1

It has been established that ROS regulate positively cellular proliferation by promoting either growth factor receptor autophosphorilation or phosphatase inactivation. Accordingly, the reduction of intracellular ROS levels by cell treatment with ROS scavenging agent can overcome the ROS-dependent up regulation of Cyclin D1 and the reduced cell capacity to exit from proliferative cycle [29].

To test the effect of yeast avenanthramides on the regulation of Cyclin D1, we performed real-time PCR assays in Yav treated HeLa and MEF cells (Figure 8A,B). Compared with the control, treatment with 100 and 150 μM Yav I significantly reduced Cyclin D1 expression levels (62% reduction average) in HeLa cells (Figure 8A) ($p<0.05$). An analogous decrease was observed in response to cell treatment with 100 μM Yav II, while following treatment with Av B no significant effect was detected (Figure 8A). Consistently, a significant reduction in Cyclin D1 expression levels was observed upon treatment of MEF cells with 150 μM Yav I and 100 μM Yav II (Figure 8B).

3.6 Yavs revert the down-regulation of FoxO1 and SOD2, and the up-regulation of Cyclin D1 caused by KRIT1 loss-of-function

Previously, we found that KRIT1, a protein involved in the human genetic disease Cerebral Cavernous Malformation (CCM), regulates the intracellular ROS homeostasis to prevent oxidative cellular damage through an antioxidant pathway involving FoxO1 and SOD2, suggesting a novel mechanism for CCM pathogenesis and opening new therapeutic perspectives [29].

Remarkably, using KRIT1$^{-/-}$ MEFs (K$^{-/-}$) and KRIT1$^{-/-}$ MEFs re-expressing KRIT1 (K9/6) [29], we

found that cell treatment with YAv can revert molecular phenotypes caused by KRIT1 loss-of-function, including the down-regulation of FoxO1 and SOD2 and the up-regulation of Cyclin D1 (Figure 9A,B), suggesting potential therapeutic benefits for CCM disease.

4 Discussion

Phenolic compounds have drawn increasing interest of nutritionists, researchers and food manufacturers due to their potent antioxidant properties, abundance in the diet, and credible effects in the prevention of various oxidative stress associated diseases, including cardiovascular diseases and cancer. Avenanthramides (Avns) are low-molecular weight, soluble phenolic compounds, composed of amide conjugates of anthranilic acid (or its hydroxylated derivatives) and hydroxycinnamic acids. These compounds have been uniquely found in oat (*Avena sativa*) where they are produced in response to plant exposure to pathogens, such as fungi, in order to counteract pathogenic effects [26]. The antioxidant, anti-proliferative, anti-inflammatory and anticancer activities of oat Avns have been demonstrated both *in vitro* and in animal models [24, 25, 34, 35].

Previously we set up a yeast based system for the production in flasks of oat avenanthramide analogous compounds, namely N-(E)-*p*-coumaroyl-3-hydroxyanthranilic acid (Yeast avenanthramide I, Yav I) and caffeoyl-3-hydroxyanthranilic acid (Yeast avenanthramide II, Yav II) [23]. The structures of the new compounds synthesized in the recombinant yeast differ from avenanthramides in the position of the hydroxyl group in the anthranilic part.

Avn content in oat greatly varies according to genotype, cultivation and storage conditions: estimates of total Avn in hulled oats range from 0.003 to 0.008% dry weight in bran-depleted oat flour, to values of 0.01-0.04% in bran-rich milling fractions. Avn concentration is also strongly dependent on growing environment, as environmental stresses play a role in inducing avenanthramide synthesis. In contrast, production of avenanthramides from yeast may allow a higher synthesis efficiency and products formation rate, a constant quality of the final product, shorter production times and lower economic cost for production process.

We report a production system, based on the growth of strain 4CL-HCT in 15L fermenter, which allowed us to obtain a final yield of 120 mg/l for Yav I and 22 mg/l for Yav II (Figure 2). This yield is 6 fold higher than that obtained with previously reported culture conditions [23].

To understand how avenanthramides gain access to cells, various methods, mainly based on the intrinsic fluorescence properties of avenanthramides, have been developed, including fluorescence microscopy, flow cytometry, and spectrofluorimetry. Indeed, in previous works [36, 37] confocal imaging was used to exploit avenanthramide auto-fluorescence and localize its synthesis in oat tissues upon helicitation. Since there is only a slight structural difference between naturally occurring avenanthramides and yeast avenanthramides, we hypothesized that Yav I and Yav II could exhibit autofluorescence as well. Confocal microscopy analyses showed that Yavs are indeed auto-fluorescent when excited at 405 nm, which allowed us to demonstrate their capacity to enter HeLa cells and localize to the cytoplasm (Figure 4). A similar localization was also reported for taxol, a natural product responsible for cell cycle arrest and used as a chemotherapeutic agent, and resveratrol [38, 39]. Avenanthramides are small metabolites with a molecular weight of around 250-350 g/mol and are soluble in alcohol and mixtures of water and organic solvents. Their penetration inside the cell could occur by either diffusion across the membrane [40] or binding to a transporter on the cell surface. These features would suggest that Yavs could diffuse in the nucleus as well, but no nuclear localization was detected in our experiments. We therefore propose that either Yavs bind to cytoplasmic targets, which prevent them from diffusing to the nucleus, or that metabolisation occurs before detectable Yav levels can be found in the nucleus.

In our previous work we found that Yav I and Yav II are endowed with a significant antioxidant activity [23]. Taken together with structural similarity, this finding raised the possibility that Yavs have bioactive properties similar to those reported for oat Avns. To verify this hypothesis we performed experiments aimed at addressing the effects of Yavs on major antioxidant and antiproliferative cell regulatory pathways.

Oxidants and oxidative stress are thought to be important contributing factors in the development of cancer and cardiovascular diseases. It is now well established that physiologic concentrations of ROS are involved in the redox-dependent regulation of multiple signal transduction pathways to fulfill a

wide range of essential biological processes, including cell adhesion, migration, proliferation, differentiation and survival. Oxidative stress may occur as a consequence of an endogenous imbalance between the production of ROS and the ability of cellular anti-oxidant mechanisms to prevent ROS accumulation. FoxO proteins are central regulators of cell homeostasis, responding to a variety of endogenous and environmental stimuli, including oxidative stress and growth factors [41]. Indeed, FoxO proteins protect cells from oxidative stress by lowering intracellular ROS levels mainly through the up-regulation of SOD2 [42, 43]. This enzyme belongs to the superoxide dismutase (SOD) protein family, which protects cells via the scavenging of the superoxide anion, a precursor of all reactive oxygen species, including the powerful oxidants hydrogen peroxide (H_2O_2), peroxynitrite ($OONO^-$) and hydroxyl radical ($^{\cdot}OH$).

To test the effect of Yavs on the regulation of cell antioxidant defense mechanism, we performed real-time PCR and Western blotting analysis of master regulators of cell antioxidant responses, including the major antioxidant protein SOD2 and its transcriptional regulator FoxO1. The experimental outcomes showed that Yavs positively regulate cell antioxidant defense mechanisms through the up-regulation of FoxO1 and SOD2 expression levels (Figure 5, 6, 7). However, differences in Yav dose-response effects in HeLa and MEF cells were also observed. Besides the possibility that a differential uptake of YAvs by HeLa and MEF cells may occur, a plausible explanation for this apparent discrepancy may lie in the dose- and cell context-dependent double-edged effects of most exogenous antioxidants, including vitamins, carotenoids and polyphenols. Indeed, there is clear evidence that exogenous antioxidants can exhibit dose-dependent biphasic effects on oxidative metabolism and redox-sensitive signaling pathways, including dose-dependent antioxidant or prooxidant and stimulatory or inhibitory effects, as well as that different conditions within distinct cell types may alter the effects of antioxidants. Furthermore, double-edged effects of antioxidants may also occur independently from their (anti-) oxidative properties [33].

Among all concentrations tested, treatment with 100 μM showed the greatest effect in term of gene

up-regulation. Notably, our results highlighted that Yavs possess a better potentiality than natural avenanthramides (such as Av B) in regulating antioxidant mechanisms through SOD2 and FoxO1 up-regulation. The correspondence in the expression profiles of these two genes, which was observed both in MEF and HeLa cells, is likely due to the well-established role of FoxO1 as transcriptional regulator of SOD2. On the other hand, the finding that master regulators of the antioxidant response, such as FoxO1 and SOD2, are up-regulated by Yavs suggests that the previously reported antioxidant activity of these compounds [23] relies on their capacity to modulate an antioxidant pathway involving FoxO1 and SOD2. Consistently, there is evidence that supplementation of rat diets with Avn extracts induces increased SOD and glutathione peroxidase activity [26].

The transcriptional factor FoxO1, a master regulator of cell responses to oxidative stress, is regulated by multiple signaling pathways acting at both transcriptional and post-translational levels [29]. In particular, central to the regulation of FoxO1 level/activity is a complex post-translational mechanism that regulates its nucleo-cytoplasmic shuttling and proteasomal degradation. Intriguingly, oxidative stress has been shown to regulate most of the FoxO1 post-translational modifications involved in the modulation of its expression levels and functions, including phosphorylation, acetylation, ubiquitination and interactions with other proteins. In turn, posttranslational control of FoxO1 can influence FoxO1 transcription [29]. In addition, there is evidence that SOD2 expression can be potentiated by mechanisms involving redox-sensitive FoxO1 interactors, including SIRT1, a redox-sensitive protein that is post-translationally modified by oxidants [29]. Taken together with these considerations, our results suggest that Yav may promote the up-regulation of FoxO1 and SOD2 levels mainly by modulating redox-sensitive post-translational regulatory mechanisms.

There is evidence that cell proliferation pathways are redox sensitive as well as that antioxidants can suppress cell hyper proliferation. Since Yavs have been shown to exert antioxidant activity, it was expected that this activity could affect biomarkers of cell proliferation. Indeed, consistently with the previously reported effectiveness of the antioxidant N-acetylcysteine (NAC) in modulating Cyclin

D1 levels [29], a clear down-regulation of Cyclin D1 expression levels was observed upon cell treatments with 100 μM Yav I and Yav II, which were significantly more effective than treatments with the same concentration of Av B (Figure 8), suggesting that Yavs might be more effective than Av B in reducing cell proliferation. Consistently, the antiproliferative activities of distinct natural avenanthramides may differ due to differences in the underlying molecular mechanisms [27, 28]. Interestingly, in the light of existing evidence that natural avenanthramides from oats exhibit anti-proliferative activity towards human cancer cells, including but not limited to colon cancer cells, our finding that Yavs can down-regulate Cyclin D1 expression more effectively than AvB suggests potential implications for cancer prevention and treatment, which deserves future specific investigation in distinct cancer cell lines.

Taken together our findings suggest that Yavs exert a cell protective effect facilitating the down-regulation of Cyclin D1 levels required from cell transition from proliferative growth to quiescence by preventing the accumulation of intracellular ROS through the modulation of FoxO1 and SOD2 levels. Further studies are required to better define the likely complex molecular machinery that mediates molecular and cellular effects of Yavs.

Intriguingly, the finding that cell treatment with YAv can revert molecular phenotypes caused by the loss of KRIT1, a protein involved in the human genetic disease Cerebral Cavernous Malformation (CCM) [29], including the down-regulation of FoxO1 and SOD2 and the up-regulation of Cyclin D1, suggests that these compounds are endowed with biological properties relevant to biomedical applications, opening a novel interesting avenue for future investigations.

Conclusions

Taken together, our results demonstrate that Yavs may enter the cell and modulate master regulators of cell antioxidant responses, pointing to potential health-promoting benefits.

In particular, our finding that YAvs are effective in rescuing molecular phenotypes associated with CCM disease suggests potential implications for prevention and treatment of this major cerebrovascular disease. Consistently, whereas pharmacological treatment for CCM disease is not yet available, the putative effectiveness of compounds endowed with antioxidant properties in preventing CCM disease onset and progression has been recently suggested [29, 44, 45]. Future focused investigations should help pursuing this promising research avenue.

In addition, taken together with the well-established health benefits of natural avenanthramides from oats, which have been attributed to their antioxidant, anti-inflammatory, and anti-proliferative activities, our finding that YAvs show better bioactivities than AvB, the original natural avenanthramide in oat, suggests potential implications for prevention and treatment of various human diseases, including cardiovascular and inflammatory diseases and cancer. These potential biologically relevant properties will be further investigated in specific cellular and animal models. Indeed, if the biological properties of yeast avenanthramides confirm to be comparable or even superior to those of natural oat avenanthramides, the yeast-based production system described here would surely represent an attractive option for the production of these molecules compared to extraction from plant tissues or chemical synthesis, providing novel, reliable and safe plant secondary metabolites for biomedical applications.

Acknowledgments

The authors kindly thank Anna Maria Milani (University of Turin) for her excellent technical assistance. Research was financially supported by FIRB 2010 project “Development of a yeast-based system for the production of novel antioxidative phenolic amides with biological properties relevant to human health” financed by Italian Minister of University and Scientific Research (MIUR).

Table 1

List of primers used for qPCR analysis

Gene	Primer Forward	Primer Reverse
GAPDH HUMAN	5'- TGCACCACCAACTGCTTAGC	5' - GGCATGGACTGTGGTCATGAG
GAPDH MOUSE	5' - ATGGCCTTCCGTGTTCCTAC	5' - GCCTGCTTCACCACCTTCTT
FOXO1 HUMAN	5' - AAGCAATCCCGAAAACATGG	5' - GGTGAGGACTGGGTCGAAAC
FOXO1 MOUSE	5' - CTTCAAGGATAAGGGCGACA	5' - GACAGATTGTGGCGAATTGA
SOD2 HUMAN	5' – CTGGACAAACCTCAGCCCTA	5' - TGATGGCTTCCAGCAACTC
SOD2 MOUSE	5' - GACCCATTGCAAGGAACAA	5' - GTAGTAAGCGTGCTCCCACAC
CYCLIN D1 HUMAN	5'- GACCTCCTCCTCGCACTTCT	5' - GAAGATCGTCGCCACCTG
CYCLIN D1 MOUSE	5'-TCTTTCCAGAGTCATCAAGTGTG	5' - GACTCCAGAAGGGCTTCAATC

Table 2

Growth parameters of *S. cerevisiae* strain carrying pESC-URA-4CL-HCT vector

	OD_{600}	**Number of cells/ml**	**Fresh Cell Weight (g/l)**	**Dry Cell Weight (g/l)**
Incubation with *p*-coumaric acid	65,7	$3,1\ 10^8$	39,7	8,1
Incubation with caffeic acid	65,1	$3,7\ 10^8$	43,8	8,6

FIGURE LEGENDS

Figure 1 - Molecular structure of yeast avenanthramides. (A) N-(E)-*p*-coumaroyl-3-hydroxyanthranilic acid (Yeast avenanthramide I, Yav I) and (B) N-(E)-caffeoyl-3-hydroxyanthranilic acid (Yeast avenanthramide II, Yav II) produced by *S. cerevisiae* expressing 4CL and HCT.

Figure 2 - Production of yeast avenanthramides Yeast avenanthramides (Yav I and YAv II) content during fermentation of *S. cerevisiae* strain carrying pESC-URA-4CL-HCT vector. Fermentation took place in a 15 L fermentor with YPGal as fermentation medium. Samples were collected periodically for extraction to determine the formation of compounds. Values are expressed as mg/L.

Figure 3 - Effect of yeast avenanthramides on cell viability. HeLa cells were seeded in 96 well plates (5000 cells/well) and treated with Yav I, Yav II or Av B at the indicated concentrations (25 µM, 50 µM, 100 µM, 150 µM). Cells treated with 0.15% DMSO were used as control (CTR). Following MTT incubation, absorbance was measured at 550 nm. Results are a mean of three independent experiments. Data were normalized for each experiment and treatment differences were analyzed by Student's *t*-test. Data are presented as mean ± SD and differences were considered significant at $p<0.05$.

Figure 4 - Yavs enter the cells and accumulate into cytosolic regions. Yav II uptake in HeLa cells as revealed by confocal fluorescence microscopy imaging. HeLa cells incubated with 150 µM Yav II displayed a strong cytoplasmic accumulation of Yav II fluorescence (arrowheads), which was excluded from the nucleus (n), reached a maximum after 2 h (A, B), and lasted for more than 24 h (C, D), although at progressively reduced intensities. Projections of multiple optical sections are

presented in A and C, and overlayed to the corresponding bright field images in B and D. Bars = 30µm.

Figure 5 - Yavs trigger the expression of master regulators of cell antioxidant responses: effect on SOD2 mRNA expression. HeLa (A) and MEF (B) cells grown to confluence were either mock-treated (CTR) or treated with different concentrations of avenanthramides (Yav I, Yav II or Av B). RNA was isolated and analyzed by RT-qPCR for SOD2. GAPDH was used as an endogenous control for RT-qPCR normalization. Results are expressed as relative mRNA level units referred to the average value obtained for untreated cells, and represent the mean (± SD) of three independent experiments. *P<0.05 versus DMSO treated cells.

Figure 6 - Yavs trigger the expression of master regulators of cell antioxidant responses: effect on FoxO1 mRNA expression. HeLa (A) and MEF (B) cells grown to confluence were either mock-treated (CTR) or treated with different concentrations of avenanthramides (Yav I, Yav II or Av B). RNA was isolated and analyzed by RT-qPCR for FoxO1. GAPDH was used as an endogenous control for RT-qPCR normalization. Results are expressed as relative mRNA level units referred to the average value obtained for untreated cells, and represent the mean (± SD) of three independent experiments. *P<0.05 versus DMSO treated cells.

Figure 7 - Yavs trigger the expression of master regulators of cell antioxidant responses: effect on SOD2 and FoxO1 protein expression. HeLa (A; B) and MEF (C, D) cells grown to confluence were either mock-treated (CTR) or treated with different concentrations of avenanthramides (Yav I, Yav II or Av B). Cells were then lysed and analyzed by Western blotting with anti-FoxO1 and anti-SOD2 antibodies. A,C) Representative Western blot analysis of FoxO1 and SOD2 expression levels.

Tubulin (α-Tub) was used as loading control. In FoxO1 blots, the upper and lower bands correspond to the phosphorylated and unphosphorylated forms of FoxO1, respectively. B,D Histograms showing quantitative results of Western blotting analysis of the relative FoxO1 and SOD2 expression levels. Optical density values are expressed as relative protein level units referred to the average value obtained for DMSO-treated cells (CTR), and represent the mean (±SD) of n ≥ 3 independent Western blotting experiments. *P<0.05 versus DMSO treated cells.

Figure 8 - Yavs promote the down-regulation of Cyclin D1. HeLa (A) and MEF (B) cells grown to confluence were either mock-treated (CTR) or treated with different concentrations of avenanthramides (Yav I, Yav II or Av B). RNA was isolated and analyzed by RT-qPCR for Cyclin D1. GAPDH was used as an endogenous control for RT-qPCR normalization. Results are expressed as relative mRNA level units referred to the average value obtained for DMSO-treated cells (CTR), and represent the mean (± SD) of three independent experiments. *P<0.05 versus DMSO treated cells.

Figure 9 - Yavs can revert the down-regulation of FoxO1 and SOD2, and the up-regulation of Cyclin D1 caused by KRIT1 loss-of-function. KRIT1$^{-/-}$ MEFs (K$^{-/-}$) and KRIT1$^{-/-}$ MEFs re-expressing KRIT1 (K9/6) grown to confluence were either mock-treated or treated with 100 μM Yav I. Cells were then lysed and analyzed by either RT qPCR (A) or Western blotting with anti-FoxO1 antibodies (B). In (A), RT qPCR data are shown as relative mRNA expression units in YAv treated versus untreated samples normalized to unity. In (B), Tubulin was used as loading control. *p<0.05 versus untreated cells. Histograms show quantitative results of Western blot analysis of the relative FoxO1 expression levels (C). Optical density values are expressed as relative protein level units referred to the average value obtained for KRIT1$^{-/-}$ cells samples and represent the mean (±SD) of n ≥ 3 independent Western blotting experiments. *P<0.05 versus KRIT1$^{-/-}$ cells.

Supplementary Figure 1. Chromatographic profile of purified yeast avenanthramides. HPLC chromatogram at 330 nm of YAv I (A) and Yav II (B) are shown for relative purity.

Supplementary Figure 2. Cell treatment with *p*-coumaric acid or caffeic acid does not result in significant intracellular fluorescence accumulation. HeLa cells were treated with 150 µM *p*-coumaric acid (A) and caffeic acid (B), two potential metabolic products of YAv I and II, respectively, and analyzed by confocal fluorescence microscopy imaging under the same experimental conditions described in Figure 4. Panel A (*p*-coumaric acid) and B (caffeic acid) show projections of multiple optical sections overlayed to the corresponding bright field images. Bars = 37.5µm.

References

1. Marienhagen, J. and M. Bott, *Metabolic engineering of microorganisms for the synthesis of plant natural products.* J Biotechnol, 2013. **163**(2): p. 166-78.
2. Du, J., Z. Shao, and H. Zhao, *Engineering microbial factories for synthesis of value-added products.* J Ind Microbiol Biotechnol, 2011. **38**(8): p. 873-90.
3. Katsuyama, Y., et al., *Synthesis of unnatural flavonoids and stilbenes by exploiting the plant biosynthetic pathway in Escherichia coli.* Chem Biol, 2007. **14**(6): p. 613-21.
4. Keasling, J.D., *Manufacturing molecules through metabolic engineering.* Science, 2010. **330**(6009): p. 1355-8.
5. Siddiqui, M.S., et al., *Advancing secondary metabolite biosynthesis in yeast with synthetic biology tools.* FEMS Yeast Res, 2012. **12**(2): p. 144-70.
6. Weusthuis, R.A., et al., *Microbial production of bulk chemicals: development of anaerobic processes.* Trends Biotechnol, 2011. **29**(4): p. 153-8.
7. Engels, B., P. Dahm, and S. Jennewein, *Metabolic engineering of taxadiene biosynthesis in yeast as a first step towards Taxol (Paclitaxel) production.* Metab Eng, 2008. **10**(3-4): p. 201-6.
8. Paddon, C.J., et al., *High-level semi-synthetic production of the potent antimalarial artemisinin.* Nature, 2013. **496**(7446): p. 528-32.
9. Dejong, J.M., et al., *Genetic engineering of taxol biosynthetic genes in Saccharomyces cerevisiae.* Biotechnol Bioeng, 2006. **93**(2): p. 212-24.
10. Westfall, P.J., et al., *Production of amorphadiene in yeast, and its conversion to dihydroartemisinic acid, precursor to the antimalarial agent artemisinin.* Proc Natl Acad Sci U S A, 2012. **109**(3): p. E111-8.
11. Koopman, F., et al., *De novo production of the flavonoid naringenin in engineered Saccharomyces cerevisiae.* Microb Cell Fact, 2012. **11**: p. 155.
12. Limem, I., et al., *Production of phenylpropanoid compounds by recombinant microorganisms expressing plant-specific biosynthesis genes.* Process Biochemistry, 2008. **43**(5): p. 463-479.
13. Vannelli, T., et al., *Production of p-hydroxycinnamic acid from glucose in Saccharomyces cerevisiae and Escherichia coli by expression of heterologous genes from plants and fungi.* Metab Eng, 2007. **9**(2): p. 142-51.
14. Branduardi, P., et al., *Biosynthesis of vitamin C by yeast leads to increased stress resistance.* PLoS One, 2007. **2**(10): p. e1092.
15. Szczebara, F.M., et al., *Total biosynthesis of hydrocortisone from a simple carbon source in yeast.* Nat Biotechnol, 2003. **21**(2): p. 143-9.
16. Park, M., et al., *Expression of serotonin derivative synthetic genes on a single self-processing polypeptide and the production of serotonin derivatives in microbes.* Appl Microbiol Biotechnol, 2008. **81**(1): p. 43-9.
17. Beekwilder, J., et al., *Production of resveratrol in recombinant microorganisms.* Appl Environ Microbiol, 2006. **72**(8): p. 5670-2.
18. Wang, Y.C., et al., *Stepwise increase of resveratrol biosynthesis in yeast Saccharomyces cerevisiae by metabolic engineering.* Metabolic Engineering, 2011. **13**(5): p. 455-463.
19. Wang, Y. and O. Yu, *Synthetic scaffolds increased resveratrol biosynthesis in engineered yeast cells.* J Biotechnol, 2012. **157**(1): p. 258-60.
20. Zhang, Y.S., et al., *Using unnatural protein fusions to engineer resveratrol biosynthesis in yeast and mammalian cells.* Journal of the American Chemical Society, 2006. **128**(40): p. 13030-13031.
21. Beekwilder, J., et al., *Valencene synthase from the heartwood of Nootka cypress (Callitropsis nootkatensis) for biotechnological production of valencene.* Plant Biotechnol J, 2014. **12**(2): p. 174-82.
22. Dai, Z., et al., *Metabolic engineering of Saccharomyces cerevisiae for production of ginsenosides.* Metab Eng, 2013. **20**: p. 146-56.
23. Moglia, A., et al., *Production of novel antioxidative phenolic amides through heterologous expression of the plant's chlorogenic acid biosynthesis genes in yeast.* Metabolic Engineering, 2010. **12**(3): p. 223-232.
24. Fagerlund, A., K. Sunnerheim, and L.H. Dimberg, *Radical-scavenging and antioxidant activity of avenanthramides.* Food Chemistry, 2009. **113**(2): p. 550-556.
25. Lee-Manion, A.M., et al., *In Vitro Antioxidant Activity and Antigenotoxic Effects of Avenanthramides and Related Compounds.* Journal of Agricultural and Food Chemistry, 2009. **57**(22): p. 10619-10624.
26. Meydani, M., *Potential health benefits of avenanthramides of oats.* Nutrition Reviews, 2009. **67**(12): p. 731-735.
27. Lee, D. and C.J. Douglas, *Two divergent members of a tobacco 4-coumarate:coenzyme A ligase (4CL) gene family - cDNA structure, gene inheritance and expression, and properties of recombinant proteins.* Plant Physiology, 1996. **112**(1): p. 193-205.
28. Gietz, R.D. and R.A. Woods, *Transformation of yeast by lithium acetate/single-stranded carrier DNA/polyethylene glycol method.* Guide to Yeast Genetics and Molecular and Cell Biology, Pt B, 2002. **350**: p. 87-96.

29. Goitre, L., et al., *KRIT1 Regulates the Homeostasis of Intracellular Reactive Oxygen Species.* PLoS One, 2010. **5**(7).
30. Balzac, F., et al., *E-cadherin endocytosis regulates the activity of Rap1: a traffic light GTPase at the crossroads between cadherin and integrin function.* Journal of Cell Science, 2005. **118**(20): p. 4765-4783.
31. Guo, W.M., et al., *Avenanthramides Inhibit Proliferation of Human Colon Cancer Cell Lines In Vitro.* Nutrition and Cancer-an International Journal, 2010. **62**(8): p. 1007-1016.
32. Nie, L., et al., *Avenanthramide, a polyphenol from oats, inhibits vascular smooth muscle cell proliferation and enhances nitric oxide production.* Atherosclerosis, 2006. **186**(2): p. 260-266.
33. Bouayed, J. and T. Bohn, *Exogenous antioxidants - Double-edged swords in cellular redox state: Health beneficial effects at physiologic doses versus deleterious effects at high doses.* Oxid Med Cell Longev, 2010. **3**(4): p. 228-237.
34. Bratt, K., et al., *Avenanthramides in oats (Avena sativa L.) and structure-antioxidant activity relationships.* Journal of Agricultural and Food Chemistry, 2003. **51**(3): p. 594-600.
35. Liu, L.P., et al., *The antiatherogenic potential of oat phenolic compounds.* Atherosclerosis, 2004. **175**(1): p. 39-49.
36. Hutzler, P., et al., *Tissue localization of phenolic compounds in plants by confocal laser scanning microscopy.* Journal of Experimental Botany, 1998. **49**(323): p. 953-965.
37. Izumi, Y., et al., *High-resolution spatial and temporal analysis of phytoalexin production in oats.* Planta, 2009. **229**(4): p. 931-943.
38. Chen, M.L., et al., *Absorption of resveratrol by vascular endothelial cells through passive diffusion and an SGLT1-mediated pathway.* Journal of Nutritional Biochemistry, 2013. **24**(11): p. 1823-1829.
39. Wong, C.C., et al., *Carrier-mediated transport of quercetin conjugates: Involvement of organic anion transporters and organic anion transporting polypeptides.* Biochemical Pharmacology, 2012. **84**(4): p. 564-570.
40. Wise, M.L., et al., *Biosynthesis of avenanthramides in suspension cultures of oat (Avena sativa).* Plant Cell Tissue and Organ Culture, 2009. **97**(1): p. 81-90.
41. Zhang, Y.Q., et al., *FoxO family members in cancer.* Cancer Biology & Therapy, 2011. **12**(4): p. 253-259.
42. Kops, G.J.P.L., et al., *Control of cell cycle exit and entry by protein kinase B-regulated Forkhead transcription factors.* Molecular and Cellular Biology, 2002. **22**(7): p. 2025-2036.
43. Nemoto, S. and T. Finkel, *Redox regulation of forkhead proteins through a p66shc-dependent signaling pathway.* Science, 2002. **295**(5564): p. 2450-2452.
44. Goitre, L., et al., *KRIT1 loss of function causes a ROS-dependent upregulation of c-Jun.* Free Radical Biology and Medicine, 2014. **68**: p. 134-147.
45. Gibson C., Z.W., Davis C.T., Bowman-Kirigin J.A., Chan A.C., Ling J., Walker A.E., Goitre L., Delle Monache S., Retta S.F., Shiu Y-T E., Grossmann A.H., Thomas K.R., Donato A.J., Lesniewski L.A., Whitehead K.J., Li D.J, *Strategy for Identifying Repurposed Drugs for the Treatment of Cerebral Cavernous Malformation.* Circulation, 2014. **in press**.

Figure 1

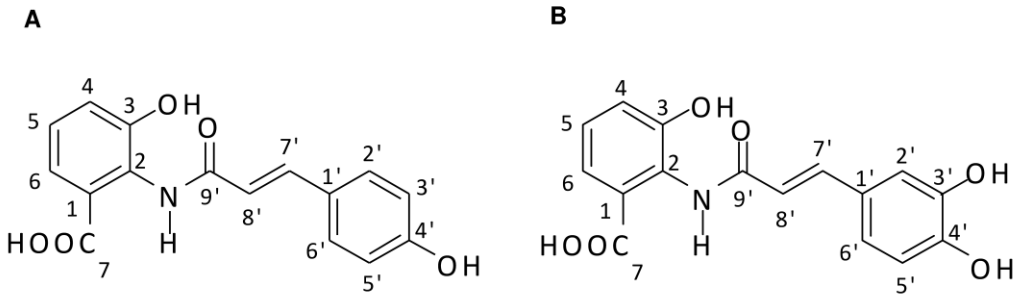

Figure 2

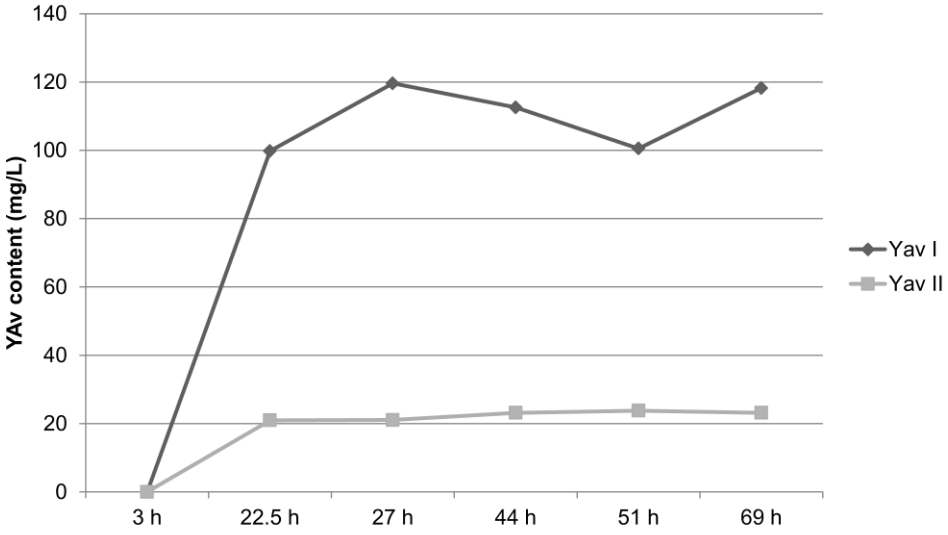
140
120
100
80
60
40
20
0
YAv content (mg/L)
3 h
22.5 h
27 h
44 h
51 h
69 h
Yav I
Yav II

Figure 3

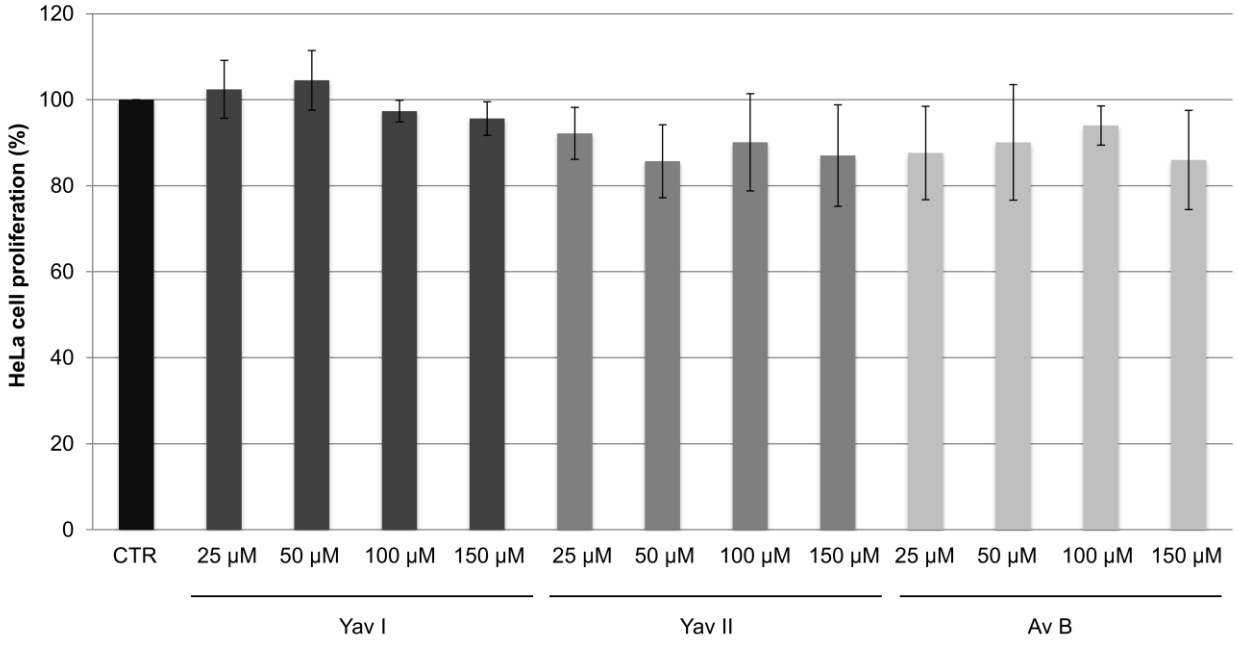
HeLa cell proliferation (%)
120
100
80
60
40
20
0
CTR
25 µM
50 µM
100 µM
150 µM
25 µM
50 µM
100 µM
150 µM
25 µM
50 µM
100 µM
150 µM
Yav I
Yav II
Av B

Figure 4

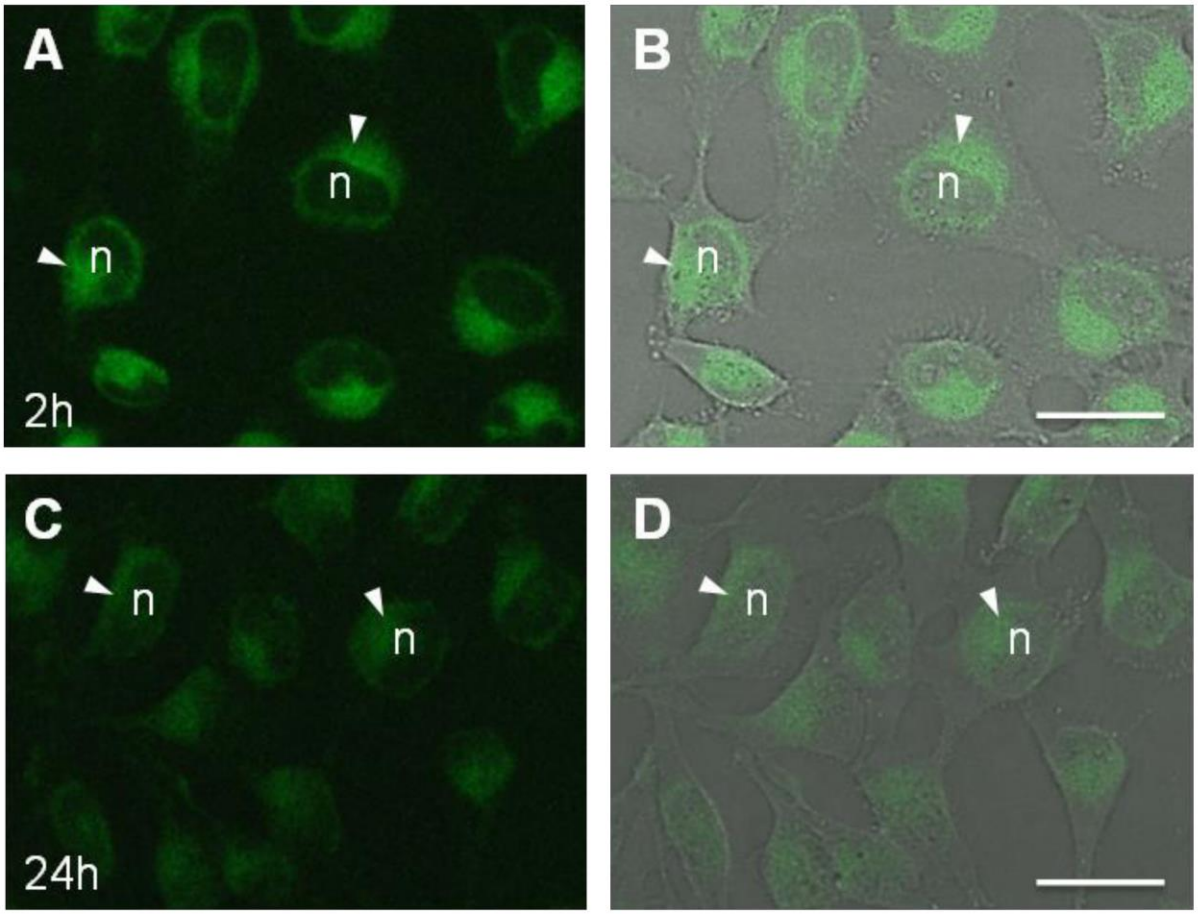

Figure 5

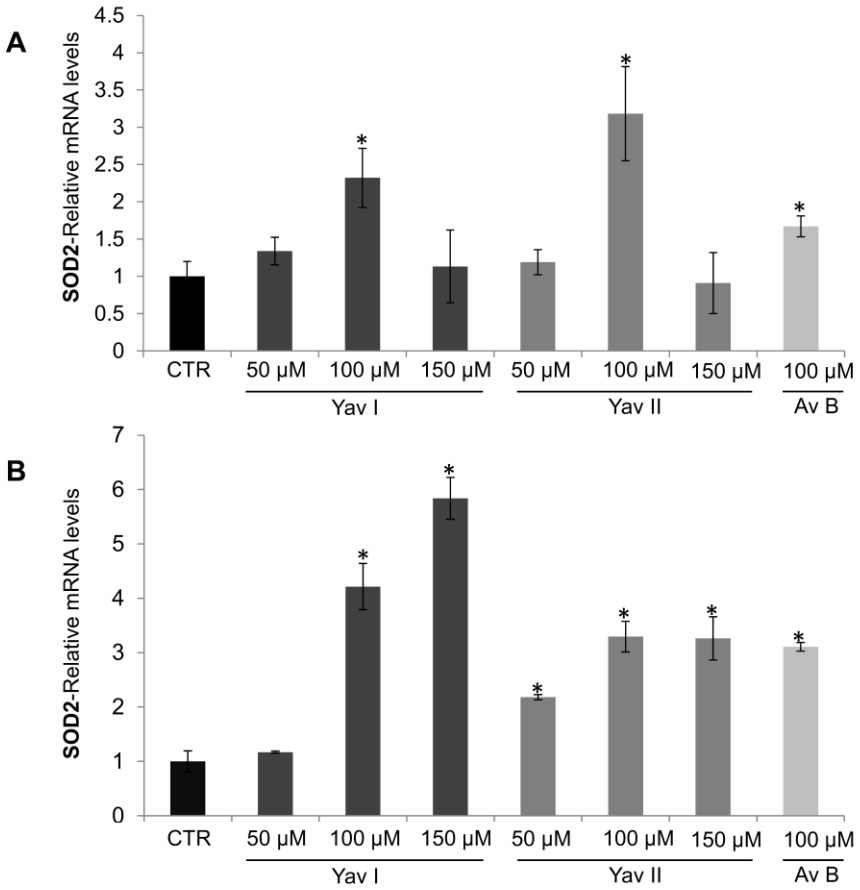
A
SOD2-Relative mRNA levels
4.5
4
3.5
3
2.5
2
1.5
1
0.5
0
CTR
50 μM
100 μM
150 μM
50 μM
100 μM
150 μM
100 μM
Yav I
Yav II
Av B
B
SOD2-Relative mRNA levels
7
6
5
4
3
2
1
0
CTR
50 μM
100 μM
150 μM
50 μM
100 μM
150 μM
100 μM
Yav I
Yav II
Av B

Figure 6

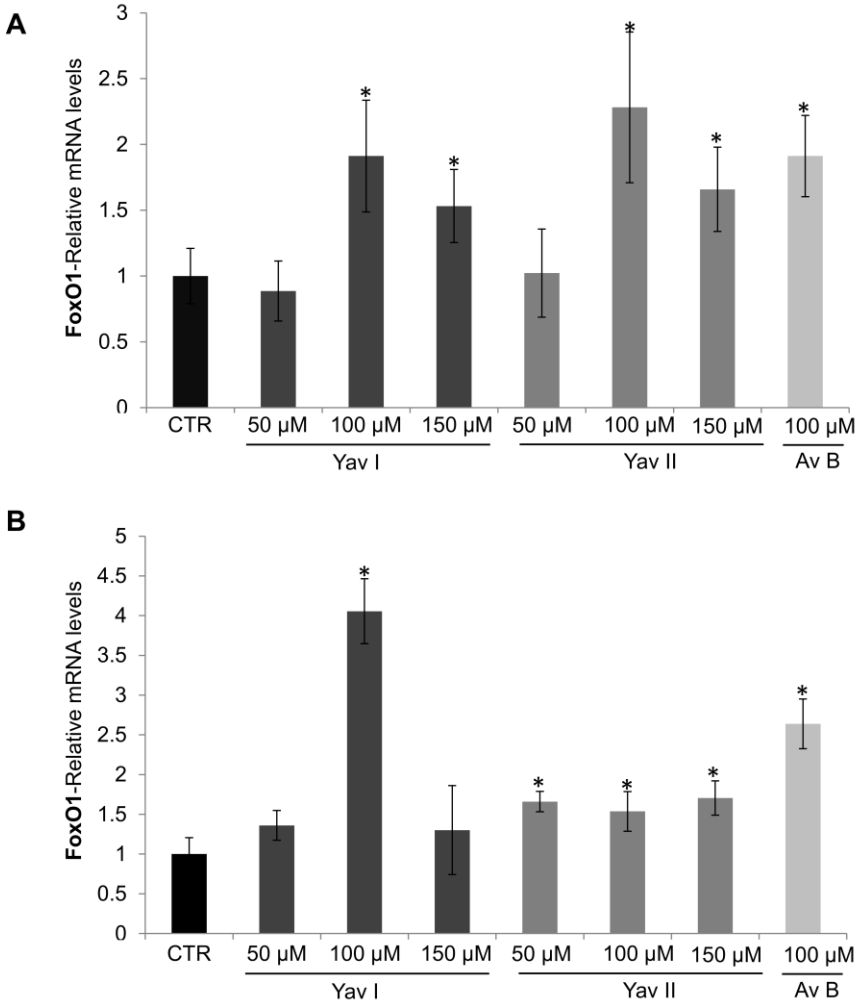
A
FoxO1-Relative mRNA levels
3
2.5
2
1.5
1
0.5
0
CTR
50 μM
100 μM
150 μM
50 μM
100 μM
150 μM
100 μM
Yav I
Yav II
Av B
B
FoxO1-Relative mRNA levels
5
4.5
4
3.5
3
2.5
2
1.5
1
0.5
0
CTR
50 μM
100 μM
150 μM
50 μM
100 μM
150 μM
100 μM
Yav I
Yav II
Av B

Figure 7

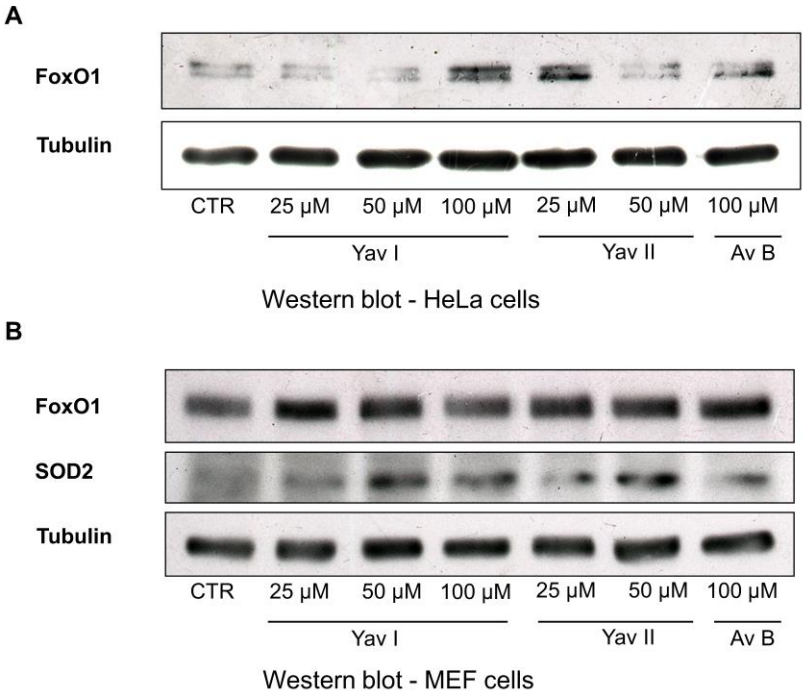
A
FoxO1
Tubulin
CTR
25 μM
50 μM
100 μM
25 μM
50 μM
100 μM
Yav I
Yav II
Av B
Western blot - HeLa cells
B
FoxO1
SOD2
Tubulin
CTR
25 μM
50 μM
100 μM
25 μM
50 μM
100 μM
Yav I
Yav II
Av B
Western blot - MEF cells

Figure 8

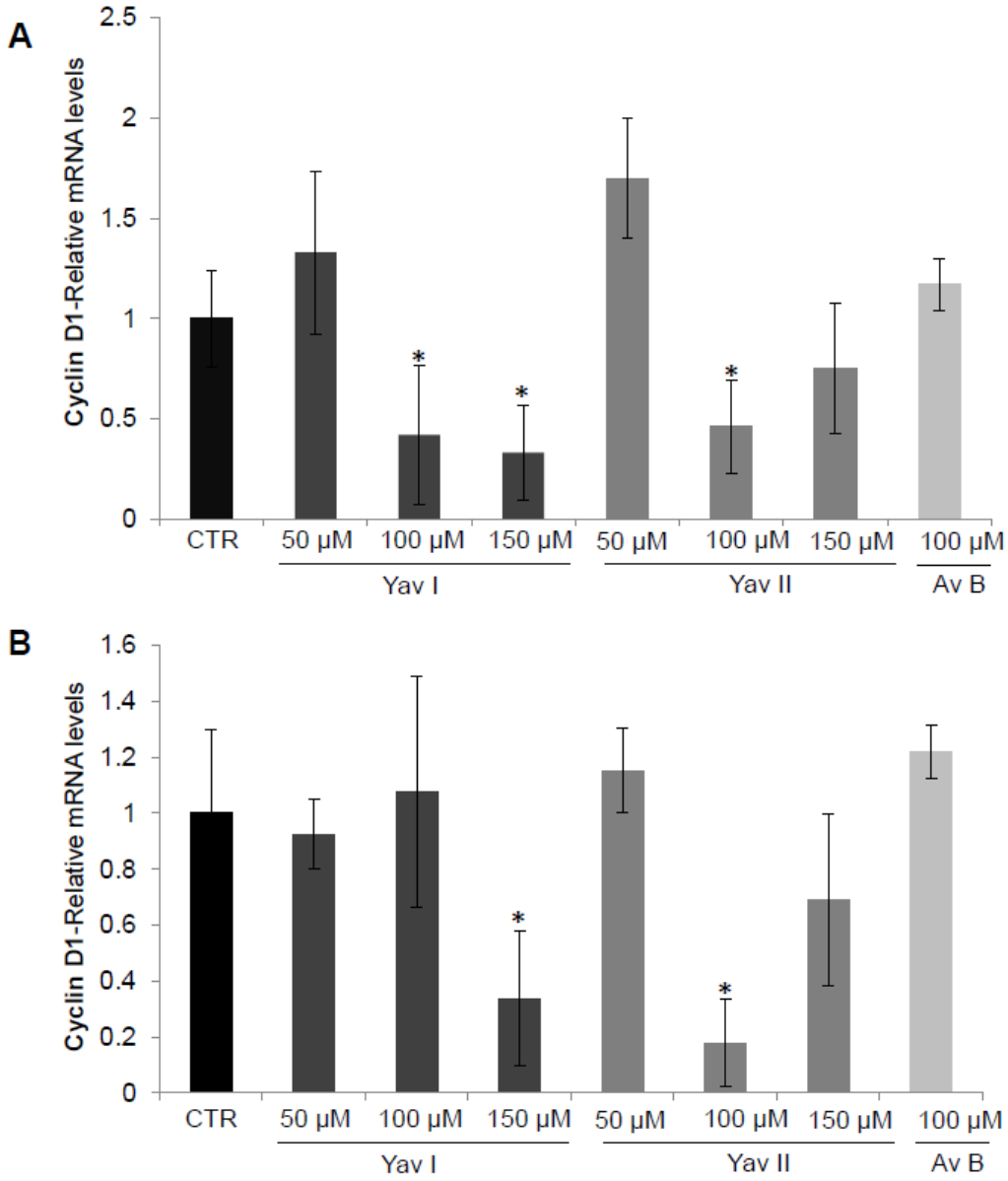
A
Cyclin D1-Relative mRNA levels
2.5
2
1.5
1
0.5
0
CTR
50 μM
100 μM
150 μM
50 μM
100 μM
150 μM
100 μM
Yav I
Yav II
Av B
B
Cyclin D1-Relative mRNA levels
1.6
1.4
1.2
1
0.8
0.6
0.4
0.2
0
CTR
50 μM
100 μM
150 μM
50 μM
100 μM
150 μM
100 μM
Yav I
Yav II
Av B

Figure 9

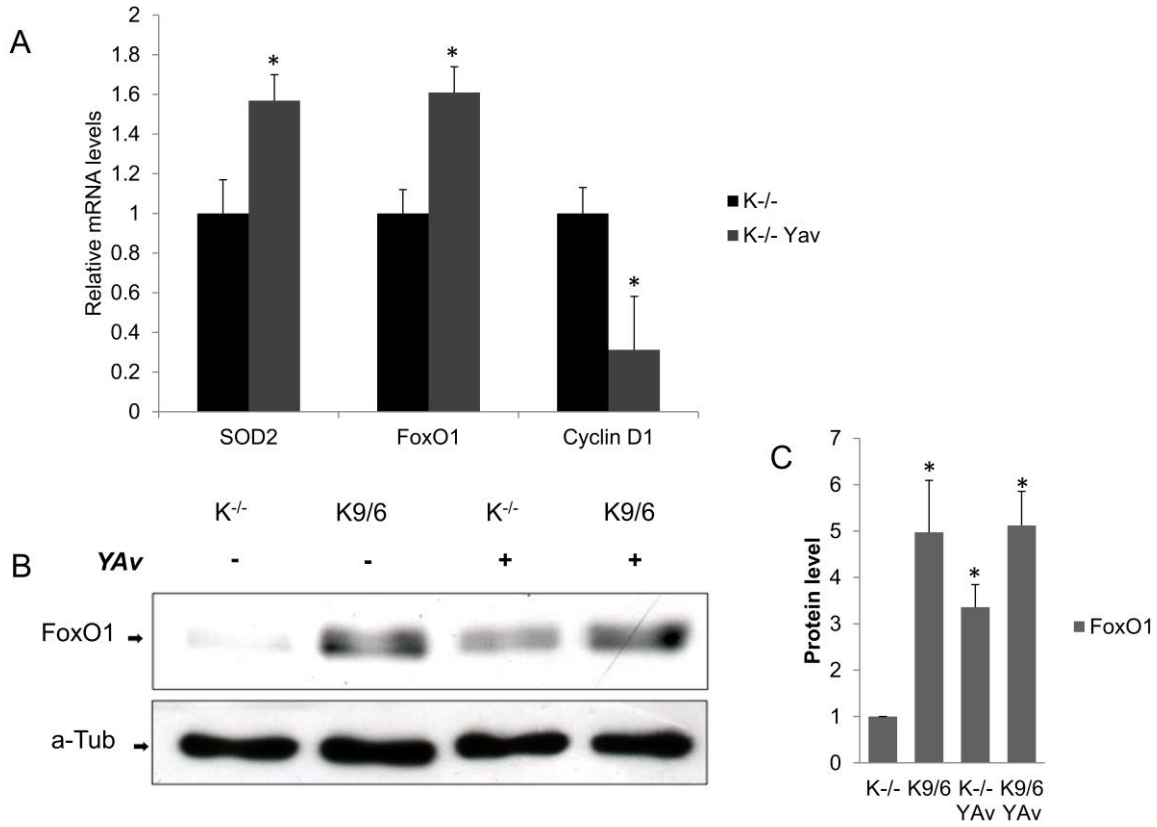
A
Relative mRNA levels
2
1.8
1.6
1.4
1.2
1
0.8
0.6
0.4
0.2
0
SOD2
FoxO1
Cyclin D1
K-/-
K-/- Yav
B
YAv
K-/-
K9/6
K-/-
K9/6
-
-
+
+
FoxO1
a-Tub
C
Protein level
7
6
5
4
3
2
1
0
K-/-
K9/6
K-/- YAv
K9/6 YAv
FoxO1

Supplementary Figure 1

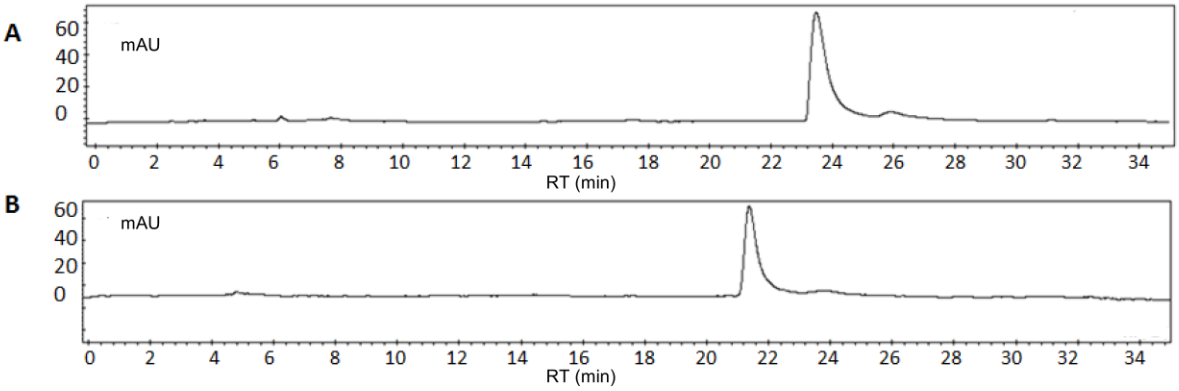

Supplementary Figure 2